Computer-Aided Design 144 (2022) 103150

Contents lists available at ScienceDirect

Computer-Aided Design

journal homepage: www.elsevier.com/locate/cad

Computation and Optimization of Structural Leaf Venation Patterns for Digital Fabrication

Sabri Gokmen

Kadir Has University, School of Architecture, Kadir Has Cd., 34083 Cibali/Fatih/İstanbul, Turkey

ARTICLE INFO

Article history:
Received 19 January 2021
Received in revised form 8 September 2021
Accepted 6 November 2021

Keywords:
Morphogenesis
Post-rationalization
Venation
Digital fabrication
Optimization

ABSTRACT

The morphogenetic design process of networking patterns produces anisotropic structural systems that can offer generative solutions for custom design applications. As an example of this type of pattern application, the leaf venation algorithm is introduced that can be customized through parametric inputs and density maps. This method is extended onto mesh surfaces incorporating multiple software applications combining aspects of parametric design, optimization and digital fabrication. The dynamic workflow is presented using a case study project titled "Calyx," a public artwork completed using the computational tools developed as part of the research. The networking structural pattern of the sculpture yielded to the development of a geometry optimization process that allowed the digital fabrication of planarized structural members. The technical aspects of the design development and post-rationalization process for the construction of leaf venations patterns are discussed.

1. Introduction

Recent developments in computational design applications have provided novel ways to integrate parametric design, optimization and fabrication of advanced structural products for architects, engineers and computational designers [1–3]. One of the key factors that characterize the internal workflow of this generative design process is the parametric variability of pre-established criteria that can be based on various structural, geometric, financial and aesthetic performances [4]. These parameters can be explored within two common methodologies that either continually transforms the generated outcome towards a desired threshold by recursively optimizing a single configuration [1], or the designer explores a population of randomly generated results that can satisfy different performance criteria for a myriad of selective and adaptive purposes [5]. In both cases, designers and engineers are often tasked with developing custom computational tools that are required for the transfer of data between software [3], developing parametric design iterations [6] and transforming geometry for various post-rationalization and fabrication processes [7].

An emerging aspect of generative design is the interactive use of multi-agent-based systems that can dynamically integrate various performance criteria or data to guide design output towards the desired configuration [8]. In this domain, generative approaches are either tested on standardized forms and surfaces or parametric component groups are transformed to find the right configurations that meet design requirements. For instance, if a parametric surface system defines the overall boundary or topology of design, then the isomorphic continuity of parts can be modified by the local transformation of geometry to meet various performance or fabrication criteria [9,10]. However, integrating the evaluated data back into the input as a feedback loop requires data transfer and optimization protocols since the input and output are reciprocally affected [8]. In contrast to parametric systems, generative applications often require pre-determined performance or geometry constraints to guide the outcome of the application [11]. To manipulate the dynamic interactions of an agent-based application, designers often use underlying isomorphic geometric inputs or data to control the behaviour of the system. In the case of parametric applications, the optimization and performance integration appears as an afterthought, whereas in the case of generative design, the data and input drive the design thought process [12].

In this paper, an example of a generative design application workflow and case study will be presented discussing the integrated use of geometry optimization on parametrically generated leaf venation patterned structural networks. This approach will be presented under the multi-disciplinary term "morphogenesis" which extends computational growth algorithms that are developed for the simulation of natural systems to a biomimetic design and construction domain [2,13,14]. In this perspective, a generative algorithm that can simulate the growth and distribution of leaf venation will be discussed that can achieve anastomotic pattern connections between growing agent trajectories [12]. This process enables parametric control for the emergent behaviour

E-mail address: sabri.gokmen@khas.edu.tr.

https://doi.org/10.1016/j.cad.2021.103150
0010-4485/

of self-organizing structural patterns while the resulting continuous networking patterns require computer-aided problem-solving protocols for design applications Mert Müldür. As a case study, a public artwork "Calyx" will be presented as a structural application of the algorithm on a hyperbolic surface while discussing the encountered issues of geometry optimization and post-rationalization for fabrication requirements.

2. Background

The digital turn has brought a myriad of computational tools to support the design and development of complex project workflows within the field of architecture and engineering [15]. As the number of technology tools has increased dramatically over the past decade, the data transfer between these programs has brought new integration problems [8]. Some of the most common issues that inter-disciplinary workflows face are the requirement of additional software that can provide efficient transfer of geometry and data simultaneously between programs offering a more robust integration for workflow efficiency. An early example of this problem resulted in the use of XML to transfer data between generative components and other design development software that was tested on stadium roof models as an application of parametric design [9]. More recently, designers started developing their own custom parametric design and data transfer tools to integrate multi-layered design criteria or satisfy various optimization objectives. Gerber et al. show the efficient use of a new prototype tool (HDS Beagle) that integrates parametric coordination between design, energy and finance to achieve multi-objective optimization [8]. Recent developments in machine learning have opened up the possibility to embed automated feedback mechanisms within the design development phase that can iterate through various optimization protocols [5]. As designers are becoming more competent programmers and complex problem solvers, new tools on data transfer and design workflow management are being introduced that outline an exciting avenue for computational research [1,3].

An emerging approach for the integration of various performative data during design generation is defined as "morphogenesis" which operates using multi-agent systems or generative algorithms that aim to satisfy various pre-defined design or fabrication criteria [13,16,17]. As a trans-disciplinary term, morphogenesis combines computation with biology by providing the exploration of performance integrated solutions and workflows for various generative design tasks [16,17]. Rather than defining an abstract or generic optimization procedure for form-finding, with this methodology designers can transfer biomimetic principles of form for the geometric description, distribution and discretization of parts [2]. Morphogenetic systems utilize simulations, parametric models, generative algorithms, and agent-based systems while integrating various structural, fabrication, construction related criteria for the parametric behaviour of parts to achieve optimal solutions [7,18]. This biomimetic process also extends the notion of self-organization in organic systems opening up the possibility of multiple feedback mechanisms to transform design and fabrication development [13].

In many contemporary architectural and art projects, computational geometry, digital fabrication and rationalization are becoming intertwined to achieve more integrated solutions to satisfy project delivery constraints [2,6,19]. Austern et al. have reviewed diverse rationalization and digital fabrication techniques in the fields of design and engineering while outlining the growing popularity and significance of parametric workflows and optimization criteria brought from materiality, fabrication and construction [1]. Parametric systems have become a popular avenue for post-rationalization and optimization protocols where design variations are evaluated using simulations and analysis to find viable solutions [20]. Post-rationalization is often considered during fabrication where geometry optimization is performed by computational tools to model how material properties constrain the geometrical configuration, manufacture, or assembly of parts [21]. An example of such geometry optimization protocol shows how the structural configuration of free-form, multi-layered architectural envelope systems could be achieved by computationally manipulating parallel mesh geometry that can provide an optimized beam layout with torsion-free nodes while presenting some limitations on finding the optimal result when the input mesh geometry is not appropriately chosen [22]. A similar application in the use of curved grid-shells presents the implication of material limitation on the design geometry following a similar process to the construction of Mannheim Multihalle by Frei Otto [6]. These approaches show that fabrication and materiality plays a key role in how the post-rationalization of design can be guided towards an achievable goal using computational tools.

Another area where design and fabrication integration requires computational workflow and tool development occurs in post-rationalization and optimization of generated geometric solutions [23]. Tepavcevic et al. presented an example in the transformation of free-form structures to planar components that could be used to build thin shell plywood structures based on friction-fit assembly procedure [19]. Mesnil et al. showed the generative use of cyclidic nets on super-canal surfaces that simplify gridshell structure geometries with planar curvature lines such as circular arcs or biarcs for form-finding [7]. A similar application in the field of architectural envelopes shows the generative placement of circular beams that can be covered with flat quads [24]. Using three design cases, Scheurer et al. highlighted the overwhelming complexity of handling design decisions with multiple objectives where optimizing everything can lead to chaos compared to emergent patterns [25]. Gerber et al. showed the potential use of an interactive framework of a multi-agent system (MAS) where designers can effectively explore their design space with informed results [8]. As the field of design and construction are becoming more integrated with technology, computational designers are being tasked with the development of new tools that can address various technical problems that emerge through dynamic project delivery workflows.

3. Morphogenesis

As a trans-disciplinary term, *morphogenesis* describes the extension of biological principles and growth mechanisms to the investigation and implementation of performative-material or generative-computational systems for various form-finding processes in design [4,13,16,25]. The translation of biological concepts is often implemented as agent-based algorithms that can mimic the behaviour of natural growth or behaviour by dynamically interacting, transforming and evolving geometric configurations of the structural form [25]. In architecture, morphogenesis has been investigated under computation, materiality and fabrication technologies to both define dynamic process-oriented form-finding strategies for generating structural configurations of form, and material strategies that are affected by selected performance criteria that meet certain fabrication restrictions or material behaviour [13,17]. With this perspective, designers utilize parametric software and programming tools to define generative workflows inspired by biological processes for the parametric investigation of a potential solution space to find forms that satisfy predefined performative criteria [25]. In recent years, these computational systems have been implemented and tested using requirements from robotic fabrication constraints [2] organic material behaviour such as the transformative capacity of wood [16],

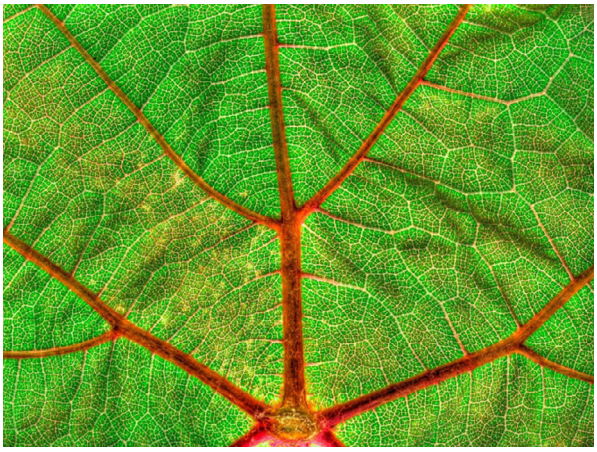

Fig. 1. Example of a reticulate leaf venation showing the hierarchical distribution of veins responsible for transportation of nutrients during growth. *Source:* Photo by Reinhold Möller, source: Wikipedia, licensed under creative commons.

construction and assembly logic [24], and digital exploration and documentation of parametric design iterations [5].

In recent years, a viable source for the implementation of morphogenetic systems in design has been botany due to the parts to the whole relationship of plants and interest in the exploration of growth mechanisms as an organic design approach [12,18]. The natural growth algorithms have been primarily explored within computer graphics with the early development of L-systems that propose a grammar-based substitution for self-replicating parts within a hierarchical graph [26]. In architecture, biomimicry has combined biology, computation, fabrication and design comprehensively to integrate data-driven protocols for various performative applications [4,12,16]. Compared to parametric design applications and engineering-based member distribution computation strategies, in biomimetic approaches, architectural geometry is developed through simulation for the determination of performative aspects of structural members. An example of this approach is the leaf venation algorithm that offers self-organizing and emergent properties for the geometric configuration of parts within a generative structural network [12]. Compared to other surface driven pattern-based approaches, the leaf venation system offers anisotropic and dynamic patterns while producing continuity and hierarchy within node networks that label it as a viable candidate for various structural applications [11,27].

3.1. Morphogenesis of leaf venation

The development of leaf venation patterns is directly correlated with the growth of the leaf blade shape that is characterized by the growth tensor field [28]. This tensor field can be described according to the location and rate of growth distributed along the leaf blade outline. The expansion of the leaf blade can be solely along the margin or distributed throughout the surface (diffused). In diffused cases, the rate of expansion can be isotropic (equal) or anisotropic (unequal) while growth tensor can be uniform or non-uniform [12,28,29]. The growth tensor field is also transformed by the vascular development of the leaf that both structurally supports and carries nutrients throughout the form. In leaves, the cellular distribution and concentration of growth hormone *auxin* are responsible for guiding the structural transformation of vascular tissue in plants during growth [30]. Auxin is spawned around the leaf blade boundary and presents changing chemical concentrations among adjacent cells. During growth, this hormone begins to be depleted and transported by cells causing some of them to be transformed into vascular tissue to become a better pathway for rapid flow of nutrients. This "canalization hypothesis" suggests that as the leaf grows the temporal modification of auxin affects how the accumulation of veins takes place, affecting both the overall topology of leaf form and structural configuration of nutrition carrying veins [30]. The cellular differentiation within plants is highly dependent on the activity, concentration and distribution of auxin that is informed by the polarity of cells, affecting the structural transformation of leaf tissue into vascular strands [31]. Auxin not only guides the transportation capacity of cells through canalization by fixing polarity but also causes structural differentiation for the development of the leaf. Furthermore, the temporal distribution of auxin plays a key role in the overall structural patterning and development of leaf venation that marks the hierarchical placement and structural thickening of veins that become a better network for fluid transportation (Fig. 1).

3.2. Computation of two-dimensional leaf venation patterns

In this section, an algorithm based on the "canalization" hypothesis using auxin distribution will be described that exhibits various performative aspects combining morphogenetic patterns with geometric parameters [30]. This investigation will be introduced and explored in two steps. In the first step, the general outline of the leaf venation algorithm developed by Runions et al. is described on a general surface that is implemented using custom gradient maps that can give control over the density of the generated anisotropic patterns [12]. In the second part, the two-dimensional algorithm is extended onto parametric surfaces to test its emergent structural networking properties. This application offers control over the emergent parametric behaviour of leaf venation using gradient maps [32] while the geometric distribution of parts is implemented as a recursive algorithm [33]. This approach advances early generative work that is limited in its geometric solution for anastomotic joints where the structural configuration of the networking pattern is thickened hierarchically for visualization purposes [11]. In this work, the same approach is further developed with computer-aided design workflow and geometry optimization protocols to transform anisotropic network patterns on mesh surfaces into thickened flat panels that can be fabricated for various architectural applications. After the general introduction of the generative workflow, the geometrical challenges presented by anisotropic structural patterns will be discussed using a case study where various computational geometry optimization protocols are established.

Runions et al. introduced the overall outline of the leaf venation algorithm discussing the robust geometric characteristics and recursive steps using a topologically enlarging leaf blade shape [12]. The computational implementation of the algorithm is developed in Processing, where the auxin sources are distributed on a region using Poisson disk sampling (PDS) [34] which are targeted by growing leaf nodes that could be placed arbitrarily. A modification to the original algorithm is the implementation of gradient maps that control the densities of the auxin sources (Fig. 2). In PDS, the sampling distances of the points are controlled by reading the alpha channel of the gradient map that corresponds with the surface space of the simulation (Fig. 2a). Darker regions assign smaller values for disk sampling radius, while in lighter areas the radii are kept large, interpolating values between low and high threshold radii. The usage of gradient maps gives some control over the density distribution of the continuous pattern, however, does not directly override the self-organizing behaviour of the generative algorithm (Fig. 2b). With this input, the density and distribution of leaf venations can be controlled that open up the possibility of various performative design applications (Fig. 2c).

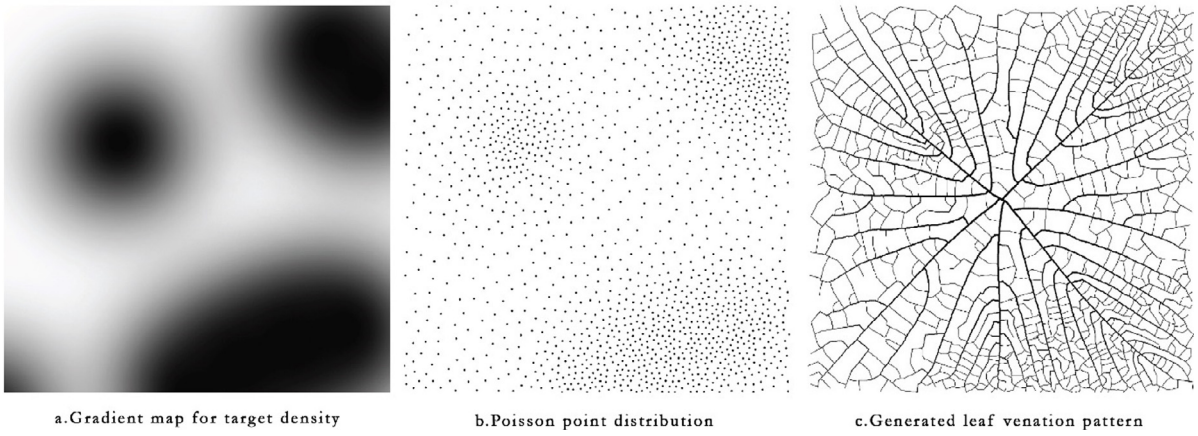

Fig. 2. The workflow of customized leaf venation algorithm in two dimensions with different densities.

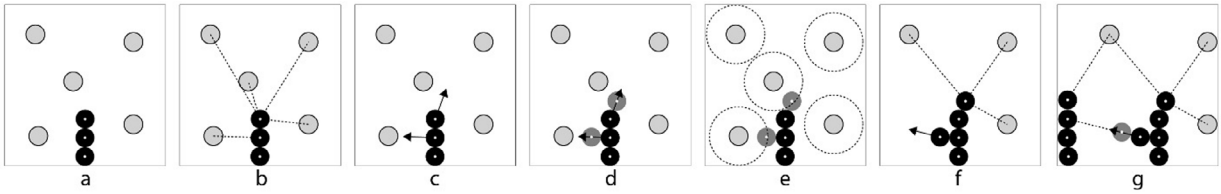

Fig. 3. Algorithmic progression of the leaf venation algorithm in two dimensions developed after Runions et al. [13]. Leaf nodes are marked as black, auxin sources are light grey. Growth directions are shown with black arrows. Target allocations are shown with dashed lines.

After the auxin sources for the venation algorithm are placed by the PDS using gradient input, the next steps for the implementation of the leaf venation algorithm on a two-dimensional surface (Fig. 3) occur in the following steps:

a. The root nodes for leaf venation growth are specified,
b. At each time step all the auxin sources are traversed and for each leaf node, the closest auxin sources are added as targets. All leaf nodes with active targets are marked as *growing*.
c. During simulation, each growing leaf node calculates the average direction to all targeted auxin sources.
d. A new vein node is added towards average direction The current node is marked as *vascular* unless it remains closest to another auxin source,
e. When a leaf node gets closer to an auxin source (*kill distance*), the source is removed from the simulation,
f. The growing nodes without auxin targets are determined,
g. The open nodes without targets acquire their new targets among non-growing leaf nodes with two connections to achieve anastomosis.

During the simulation of the venation algorithm, the steps (a–g) are repeated until all the auxin sources are exhausted and all open nodes with targets are connected. At each time step, the active leaf node connections are thickened to visualize a hierarchical venation pattern. For the algorithm, two sets of parameters are used. The first parameter, *birth distance*, defines the minimum and maximum radii used for PDS that is mapped onto auxin sources using gradient maps [12,31] (Fig. 2). The second parameter, *kill distance*, controls the threshold for auxin source removal (Fig. 3e). If the *kill distance* is low, the resulting patterns become more articulated with more leaf nodes acquiring more targets. When kill distance is high, the targets are removed more frequently and the point density plays less influence on the emerging pattern.

To produce patterns with closed loops, the growing open tips that do not have any auxin targets look for the closest leaf node in the direction of their growth (Fig. 3g). These targets are chosen within an angle threshold and connected in a few steps. The open growing tips are marked as vascular when they connect to another leaf node to create a closed-loop in the network. During this process only 3-legged "Y" joints or 2-legged "I" joints between leaf nodes are allowed to maintain a leaf venation pattern. This way the algorithm creates anastomosis among leaf nodes producing continuous anisotropic patterns reacting to gradually changing local densities.

Fig. 4 shows the animation sequence of how the anisotropic pattern is created with morphogenesis. A general property of the leaf venation algorithm is the graph output of the generated structural network that is achieved by connecting leaf nodes. The thicknesses of each node are incremented to visualize a hierarchical venation pattern over time. The algorithm terminates when all the growing leaf nodes are either connected to an acquired target node or cannot find any more sources or targets

3.3. Computation of leaf venation patterns on mesh surfaces

In the next phase, the two-dimensional leaf venation algorithm is extended on a bounded surface domain to develop a surface patterning strategy that can work on triangulated mesh surfaces. During this transfer, various surface input geometries are used to test the behaviour of the three-dimensional application of the venation algorithm. A critical aspect of the extension of the algorithm is that the surface geometry is used as a topological input that can present a parametric simulation space for the emergent behaviour of the algorithm. In this regard, the approach separates surface generation and patterning application while treating the former as a driver for the latter. The technical aspects and limitations of this implementation are discussed below.

The extension of the venation algorithm to triangulated mesh surfaces follows the overall two-dimensional implementation presented in Fig. 3. In three dimensions, surfaces are first transformed into meshes to be used as guiding geometry for the algorithm (Fig. 5). On the mesh surface, the PDS of auxin sources

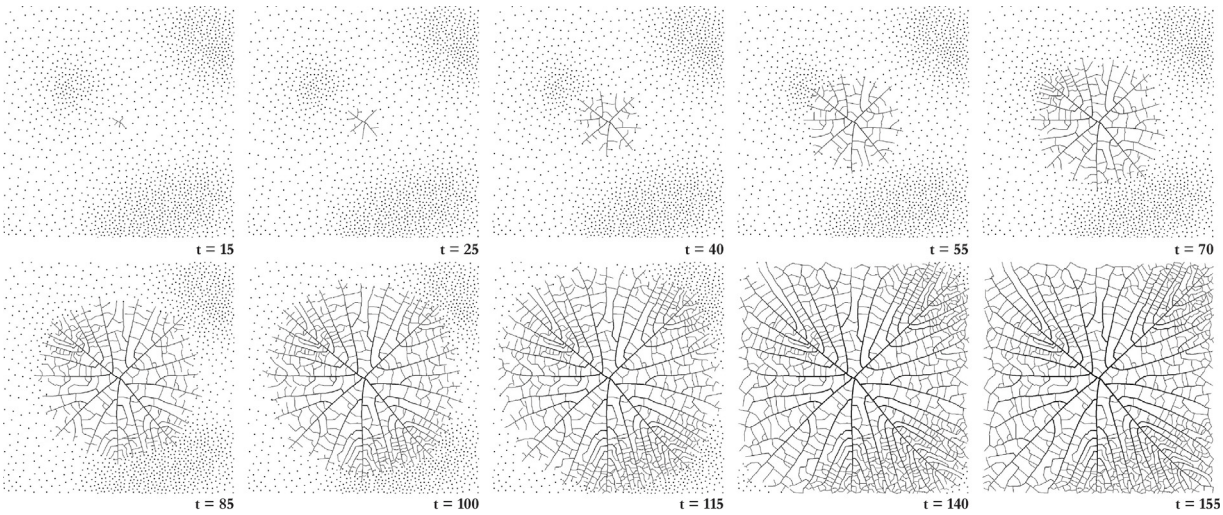

Fig. 4. Animation sequence of leaf venation algorithm running with custom density distribution (see supplementary video files for 2d tests)..

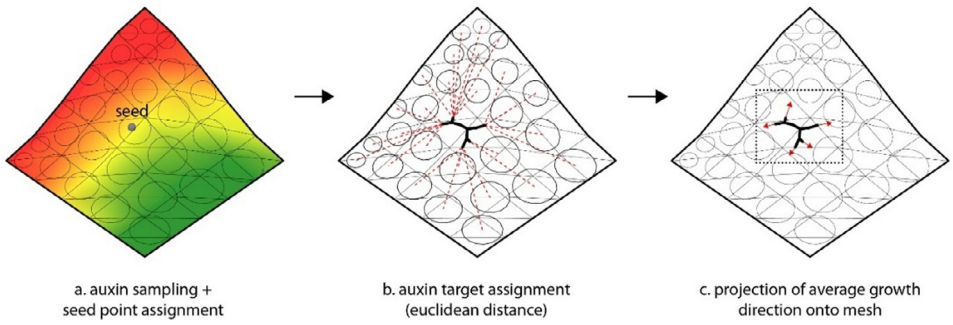

Fig. 5. Calculation steps of vein growth directions on a mesh surface.

is computed using colour gradients of mesh vertices that determine high (green) or low (red) values for radii of auxin sources (Fig. 5a). After the placement of auxin sources and determination of a seed point for growth, the two-dimensional algorithm protocol is applied. To provide computational efficiency, the calculation of targets for vein nodes is done using Euclidean distances using a distance threshold to filter points that are further apart from growing nodes (Fig. 5b). Once the average target direction is computed this vector is then projected onto the mesh to guide growth on the surface (Fig. 5c).

To control the density of the pattern, and overall attractor-based parametrization of the input mesh surface is considered where the density of point distribution can be controlled (Fig. 5a). By assigning a colour gradient to each triangle, the auxin sources are randomly populated on imported meshes in Processing. The root nodes for the veins can be placed by the user on any selected triangle. The algorithm develops a hierarchical structural outcome, with earlier nodes growing thicker geometric connections. In three dimensions, the generation stops when all the auxin targets are exhausted and open growing nodes with acquired targets are connected.

Compared to the two-dimensional implementation, when the simulation is run on meshes, numerous collision detections and direction optimization routines take place. For instance, the direction calculation from the auxin sources can point towards a direction away from the surface depending on the locations of the targets. To prevent this issue two solutions are considered. First, the auxin targets can be filtered using a distance threshold that ignores points far away from growing nodes. Secondly, the resulting average growth direction is projected onto the mesh and growth increments are kept below average mesh edge length (Fig. 5c). This way the main algorithm loop (Fig. 3a–g) runs in the same fashion and the input mesh informs the overall topology of the final leaf venation configuration.

In the three-dimensional implementation, the input mesh surface poses restrictions for the geometric modelling of venations patterns as the auxin target allocation and average direction calculation and vein node sizes can generate geometrical irregularities. A general shortcoming of the algorithm is the determination of a step size for how growth advances during simulation. If the growth increment between leaf nodes increases, then the generated structure may begin to deviate away from the guiding input surface or yield to zigzaggy behaviour (Fig. 6a). This irregularity is encountered on surfaces with high curvature changes where the algorithm fails to follow input geometry and anastomosis between growing nodes fails. This can be partially solved by projecting the average growth directions onto the mesh surface, however, the surface curvature still acts as a major determinant for how the venation pattern is generated (Fig. 6b). To avoid geometric irregularities of the pattern, the guiding geometries can be either selected from single or low curvature surfaces or growth increments are kept below surface curvature values to comply with the emergent behaviour of the venation algorithm. Initial simulation results show that the venation algorithm is extendable to three-dimensional mesh surfaces with the thickening of the venation pattern informed by the hierarchy of the emergent structure controlled by the custom parametric surface gradient (Fig. 7).

The extension of the algorithm to mesh surfaces is further investigated using various surface topologies, custom densities,

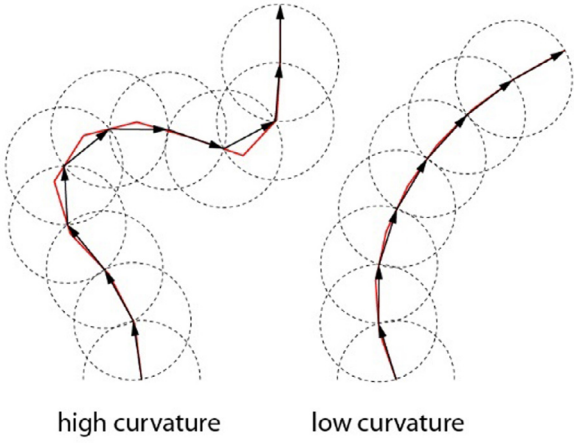

Fig. 6a. Relationship of surface curvature and growth distance of vein nodes. Surface sections (red) with high curvature values require smaller increments for growth distance to trace geometry while low or single curvature surfaces can be traced more efficiently with venation algorithm. (For interpretation of the references to colour in this figure legend, the reader is referred to the web version of this article.)

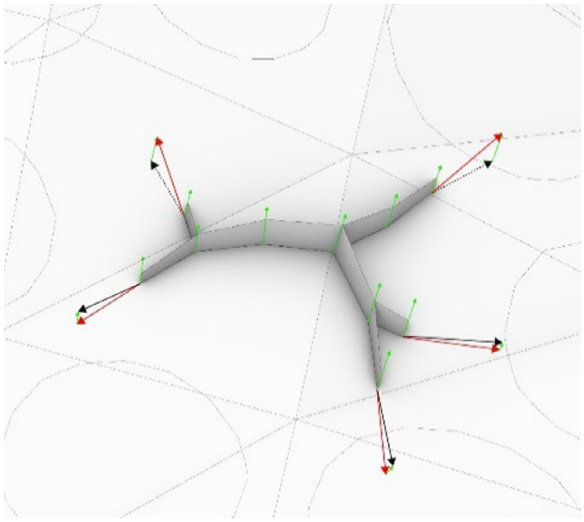

Fig. 6b. Computation of average growth directions of veins on a mesh surface (Enlarged from Fig. 5c). The average directions (black arrows) are projected onto mesh surface using mesh normal (green) to calculate growth directions (red). (For interpretation of the references to colour in this figure legend, the reader is referred to the web version of this article.)

seed points and different growth distances to investigate the dynamic relationship between venation and surface curvature (Fig. 8). The results showed the applicability of custom densities for branching morphogenesis of venation algorithm, however, surfaces with high curvature values produced pattern irregularities and collision of growing vein nodes. While the resulting venation pattern follows the input surface geometry, the algorithm shows emergent behaviour to local curvature and density changes when executed on mesh surfaces. This may result in erroneous venation configuration that may produce zigzaggy behaviour (Fig. 8s1), incomplete growth (Fig. 8s1, s3) and incorrect anastomosis (Fig. 8s2, s3, s4). Furthermore, the thickening of the venation pattern may produce imperfect connections due to the sudden change of surface normals or node thicknesses that occur during anastomosis [11]. This problem is solved in the Section 4.3 where the generated pattern is first refined as a network of lines that are thickened using a post-rationalization protocol for the emerging two and three legged node connections.

During simulation of the leaf venation algorithm on meshes, the *kill distance* is computed using Euclidean distance for simplicity and efficiency. This provides faster computation of targets during the simulation and since the directions of growth are projected onto the input mesh surface, consistent venation geometries are produced. After morphogenesis of the venation, two sets of geometries are retrieved. The first geometry is the set of twisted boxes that visualize the growing pattern, and the second geometry is the line network that connects the nodes. The former is modelled using twisting boxes that thicken the veins along the normal inherited from the mesh surface. The profiles used for thickening are also enlarged hierarchically to visualize the overall distribution of the emerging structure. The latter polyline network is used by the post-rationalization protocol to achieve thickened structural members made of planar surfaces.

4. Case study: Calyx

In this section, we will describe a public artwork project that was designed using the structural venation algorithm where the geometry output is further optimized for fabrication. The project called “Calyx” was developed as an investigation bridging biology, art, computation and fabrication and funded by the campus art program of the University of Rochester. The sculpture was developed through collaborations between designers, structural engineers, digital fabricators, and developers and was permanently installed at the University of Rochester campus in summer 2015. The development of the project is an extension of early research on leaf venation patterns [11] with the integration of a computer-aided design workflow and post-rationalization algorithm for the digital fabrication of the sculpture.

4.1. Design development workflow

To develop the sculpture for digital fabrication, an array of diverse computational tools were used. Fig. 9 shows the overall design development workflow diagram that involves digital and parametric modelling, simulation, finite element analysis, optimization and custom geometry translation tools [8,20,22,23]. The initial formal development for the structure took place in Rhinoceros and Grasshopper to prepare a quasi-hyperbolic surface by revolving an arc (W1) around a vertical axis. This surface is then transformed into a coloured mesh (W2) that is used for point density mapping as a guide for leaf venation morphogenesis. This mesh data including vertices and colours are transferred into Processing where the leaf venation algorithm is run multiple times to test the generative capabilities of the algorithm (W3). Initial morphogenetic experiments showed that the venation algorithm was efficient to produce a network of polyline curves while yielding to open structural joints where simulation failed to produce anastomosis. This occurred due to geometric constraints of either not finding an auxin target or another leaf node to connect the growing structural elements [12]. After numerous generative tests, one of the satisfactory results is chosen to be imported into Rhino, where the polyline connections were reduced to fewer nodes to simplify structural elements (W4). A key factor in the simplification of the structure was the fabrication requirements. Since the sculpture was to be positioned outdoors, all parts of the structural network were decided to be fabricated out of stainless steel sheets with optimal joints and folds, and the spaces between members needed to allow further welding and ease of access for assembly operations.

A major challenge we faced during the geometric development of the project was the “thickening” or offsetting of the

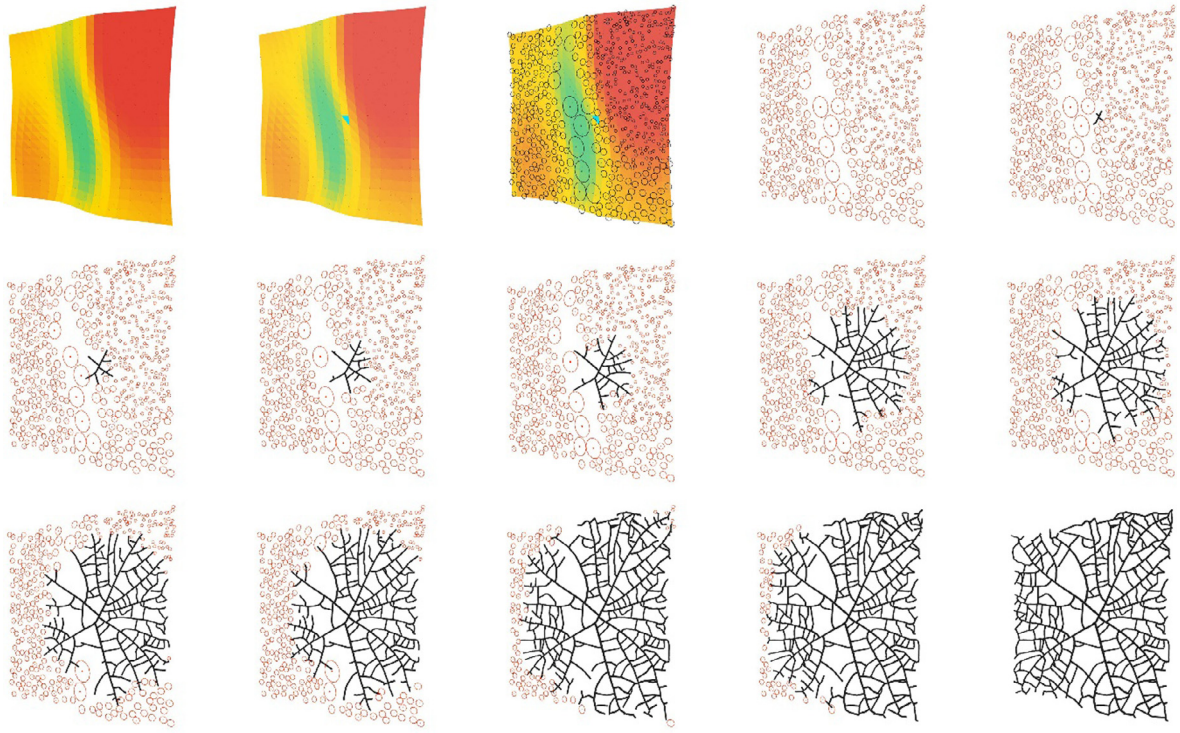

Fig. 7. The leaf venation algorithm on a 3d mesh surface showing custom densities. The auxin source distribution is customized using colour gradients that control the auxin source distribution and branching morphogenesis. Triangle marked in cyan shows the seed point. The red circles show the auxin placement and radii distribution over mesh (see supplemental material for 3d surface tests). (For interpretation of the references to colour in this figure legend, the reader is referred to the web version of this article.)

polyline structure into planar pieces. This required a computational approach that first transformed each anisotropic polygon into a Delaunay triangle mesh that captures the topology and connectivity of polygons (W5) [35]. Simultaneously, the final polyline pattern (W4) was used for finite element analysis in Matlab (W6) that resulted in hierarchical structural evaluations resembling leaf vein networks. In the final phase, the structural thicknesses from Matlab (W6) and the Delaunay triangulation specifying the location of anisotropic venation patterns (W5) were combined in a custom post-rationalization protocol developed in Wolfram Mathematica (W7) where the surface normals of over 200 nodes with 2-legged and 3-legged joints were optimized to maintain planarity requirement for thickening of the structural panels. The thickening of each node also incorporated the hierarchical structural thicknesses specified by finite element analysis (W6) [22,36]. Finally, the resulting mesh structure was imported into Rhino/ Grasshopper to model material thicknesses and colouration of the sculpture (W8).

4.2. Structural feedback

A key factor in describing the material thicknesses for structural offsets was the structural analysis applied to the final geometric graph output of the venation pattern using Matlab (Fig. 10). The structural engineer was provided with a line network of the final venation pattern and this connectivity diagram was used to calculate the optimal structural solution for the artwork that was going to be constructed using stainless steel. Since the generated structure followed the hierarchical branching development of leaves, the lower positioned central veins traversing the sculpture geometry required thicker material to support higher structural loads. Another property of the structural evaluation showed different performance between continuous longer members and anastomotic shorter parts that fill in between surfaces, the former acquiring higher loads (red), and the latter remaining thinner and uniform (yellow). All the outer offsets for flat panels were directly inherited from the minimum structural offsets. However, these thicknesses were gradually interpolated towards the top of the structure to give a continuous geometric effect while satisfying the minimum structural requirements.

4.3. Post-rationalization and geometry optimization for fabrication

The construction of free-form structures using beam and node networks for various architectural applications require the implementation of geometry optimization protocols. Using mesh geometry, the connectivity and thickening of node networks can be investigated for structural applications. In this domain, various applications have been developed ranging from mesh parallelism with edge offset meshes [22], modular standardization and rationalization of Voronoi based node networks [37] and approximating edge offsets by constructing planar hexagonal meshes for freeform surfaces [36]. In line with this research, in this section, we will describe the geometric problem of designing a network of planar panels that share common edges. A novelty of the contribution of this implementation is the parametric thickening of a non-uniform anisotropic surface pattern with two or three-legged nodes. Two algorithms for solving the geometric problem are given: (1) a numerical optimization based on an objective function, (2) a simple iterative method based on repeated vector projection [38].

4.3.1. Geometric problem

The input to our method is a polygonalized manifold with a boundary. For each input edge of a polygon, we construct a planar quadrilateral (which we will call a "panel") that includes the input edge, as well as two new adjacent edges that are contained in the line of intersection between all planes for panels

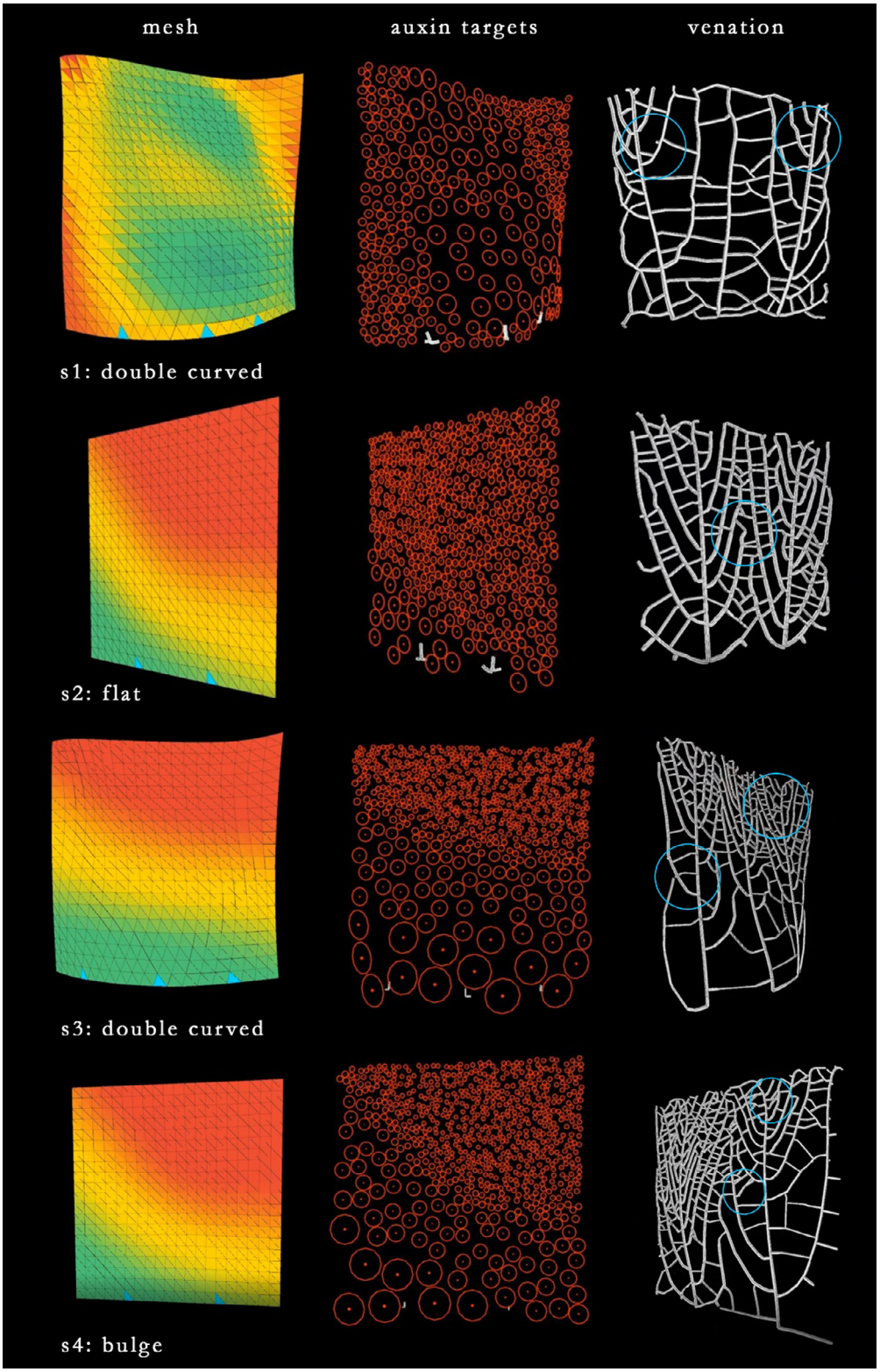

Fig. 8. Examples from surface tests showing the dynamic interplay between different surface curvatures and auxin target densities and emerging structural patterns on a surface. Erroneous configurations of venation are shown using circles in cyan colour where the algorithm generates zigzaggy behaviour (s1), incomplete growth (s1, s3) and incorrect anastomosis (s2, s3, s4) (see supplementary files for growth animations). (For interpretation of the references to colour in this figure legend, the reader is referred to the web version of this article.)

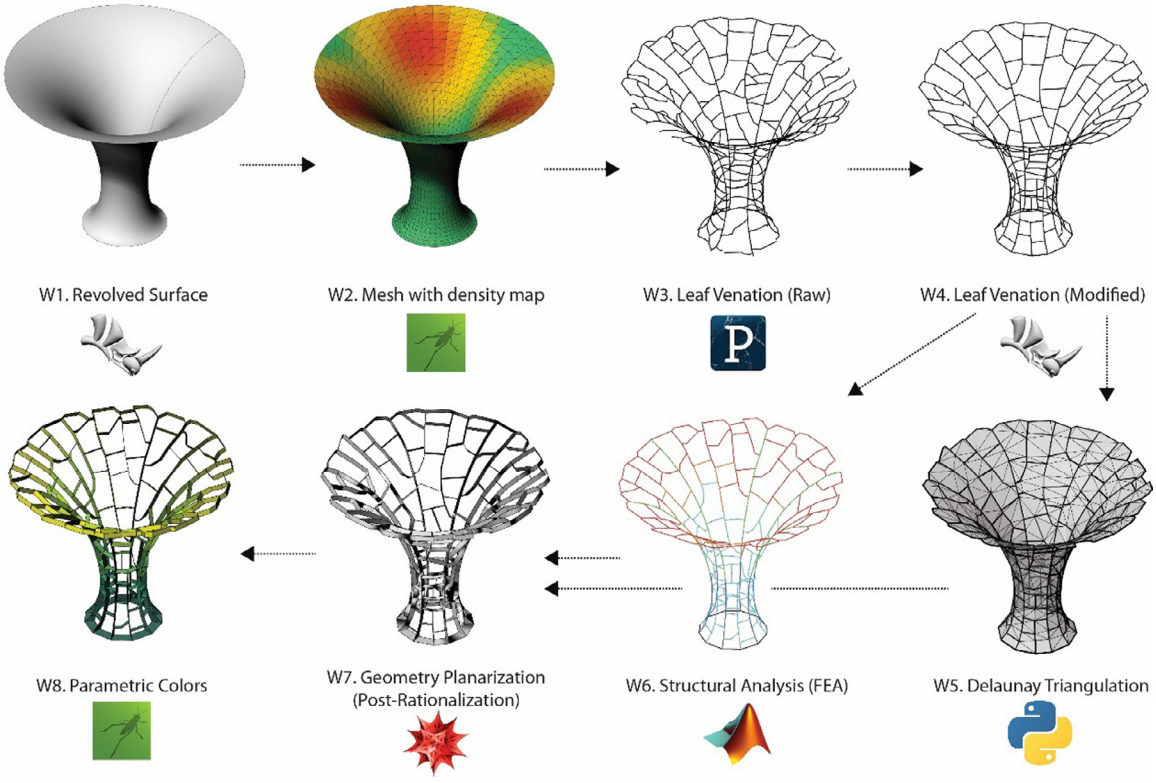

Fig. 9. Calyx sculpture development stages showing geometric transformation and computational tools (W1. Rhinoceros, W2. Grasshopper, W3. Processing, W4. Rhinoceros, W5. Python, W6. Matlab, W7. Mathematica, W8. Grasshopper).

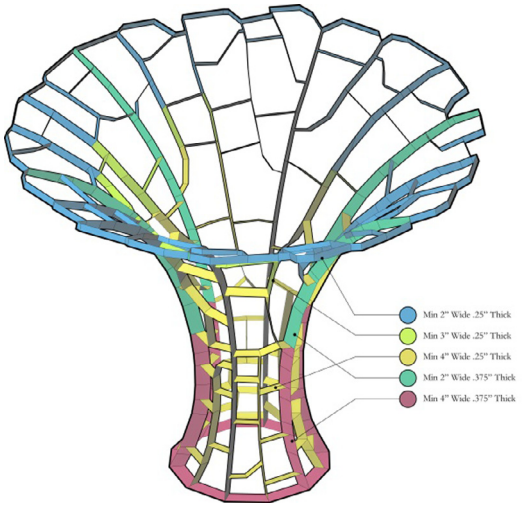

Fig. 10. Calyx structural member distribution showing the minimum material thickness and geometry offsets.

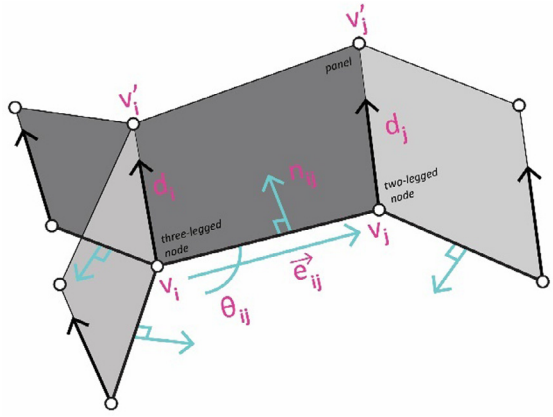

Fig. 11. Offset direction calculation for geometry optimization of node network.

incident upon the endpoints of the edge. Fig. 11 shows this configuration.

Here the panel contains the vertices: v_i, v_j, v'_j, v'_i.

For a panel to be planar it must satisfy this constraint:

$$\widehat{n_{ij}} = \widehat{d_i} \times \widehat{e_{ij}} = \widehat{d_j} \times \widehat{e_{ij}}$$

At each vertex, a height h_i can be specified. These heights do not impact the planarity of the panels, as thus are ignored during the optimization.

$$v'_i = v_i + \widehat{d_i} * h_i$$

In this problem, there are 2 free variables per input vertex and one constraint equation per edge. Thus, the problem may be over or under constrained based on the connectivity of the network. If the network is derived from the edges of a 2D manifold surface, as described in previous sections, the problem is under-constrained, and a solution always exists. Similar approaches to this problem have been previously presented showing mesh offset calculations using planar quad mesh parallelism for quadrilateral, pentagonal and hexagonal meshes [22], and using planar hexagonal meshes with arbitrary shapes [36]. In the approach shown below, an alternative numerical optimization for vertices with degrees of two and three on 2D manifold surfaces are introduced that can be solved by first developing a Delaunay triangulation of the node network to produce closed triangulated polygons that define the

connectivity of the anisotropic pattern [39]. This Delaunay triangulation is directly used for the following numerical optimization that stores the connectivity and vertex indices for each panel and closed polygon shapes of the venation pattern.

4.4. Numerical optimization

To find a solution via numerical optimization, we need an objective function that encodes the constraints (above) and any additional aesthetic criteria. For Calyx, we attempt to match each to the input surface normal d_i^0 at v_i.

We parameterize the free variables as an angle $\boldsymbol{\theta_{ij}}$ per input edge. This angle specifies a rotation of the initial panel normal around the input edge.

$$\boldsymbol{n_{ij}} = \boldsymbol{R}(\boldsymbol{\theta_{ij}}, \widehat{\boldsymbol{e_{ij}}}) \cdot \boldsymbol{n_{ij}^0}$$

where $R(\theta, \hat{e})$ is the rotation by θ radians around vector, and the initial panel normal $n_{ij}^0 = (\widehat{d_i^0} + \widehat{d_j^0})/2$.

$$min_{\theta_{ij}} \sum_{i,j} (d_i \cdot \widehat{n_{ij}} + d_j \cdot \widehat{n_{ij}}) + \alpha \sum_i \theta_i$$

where the first term penalizes non-planarity, and the second term penalizes deviation from the desired input directions. For Calyx we set $\alpha = 0.01$. To solve this optimization, we use the FindMinimum routine in Mathematica. This routine takes an initial point in the search space (in our case $\theta = 0$) and finds a local minimum. For Calyx this search completes in milliseconds.

4.4.1. Iterative method

Though the above solution is efficient, it is not simple to integrate Mathematica into our Rhinoceros

Grasshopper workflow. To provide an integrated design workflow, we implemented an optimizer in the Python language that iteratively solves for the panel normal [38]. Because this iterative solution is implemented in pure Python, without external dependencies on numerical solver libraries, it is easy to integrate with Rhinoceros.

The iterative method is as follows:

1. Initialize per-vertex directions d_i and panel normals n_{ij}.
2. Project each vector d_i onto its incident panels' planes n_{ij}.
3. Move d_i towards the average of projections.
4. Reestimate n_{ij} as the average of $n_i \times e_{ij}$ and $e_{ij} \times n_j$.
5. Repeat from step 2, until converged.

Notice that this procedure does not parameterize the free variables as a rotation per edge, but instead operates directly on the per-vertex directions and panel normals.

This procedure is slower to converge (in wall-clock time) than the Mathematica solver but produces sufficiently accurate results in <3 s on the Calyx model. Fig. 12 shows the convergence of the objective function with stepSize = 0.5 that was stopped after the error was less than 0.01 mm.

In the proposed iterative method the orientation of parts can be controlled parametrically as planarity constraints for certain joinery and pieces can be directly input by overriding the panel normal (n_{ij}). While this override was applied only for the planarity of the bottom pieces that had to be aligned parallel to the base of the structure for site anchoring, the vertical growing branches of the sculpture received their optimized orientation through the iterative method that followed the normal directions of the input geometry.

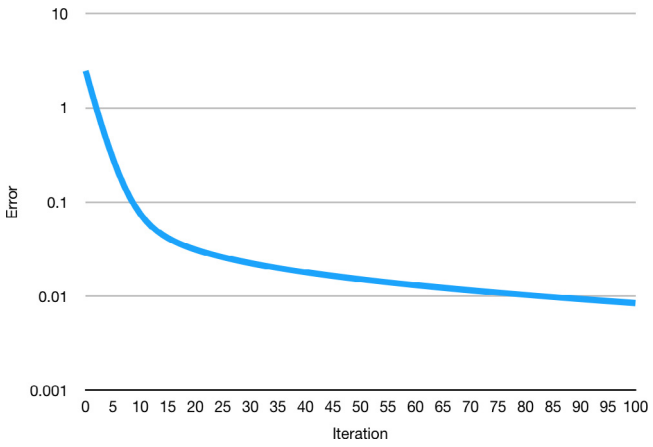

Fig. 12. Convergence of the objective function for the iterative method with stepSize = 0.5.

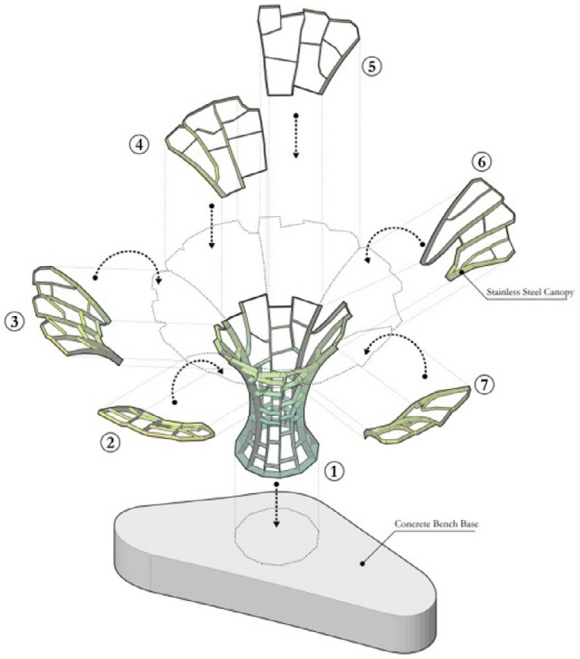

Fig. 13. Discretization of assembly groups for fabrication.

5. Construction and assembly

After the post-rationalization of the sculpture geometry, the overall form was strategically divided into seven assembly groups that are fabricated out of flat stainless steel sheets where all the separate parts were connected using welding (Fig. 13). The digital fabrication process begins by cutting all the pieces of the sculpture out of stainless steel sheets and marking them with numeric tags (Fig. 14). During the fabrication process, all the assembly groups were welded together while separate groups were held together using clippers before colour coating application (Fig. 15). This process was coordinated with the fabricator and the determination of partitions yielded to half-thickness edges where parts joined. This ensured the overall structural thickness requirements for the pieces where two halves met on part faces, as well as maintained the original hierarchical structural configuration for the artwork that required a bottom-up construction and assembly.

After the transportation of the sculpture onto the site, the central trunk piece was anchored to a foot-thick concrete base

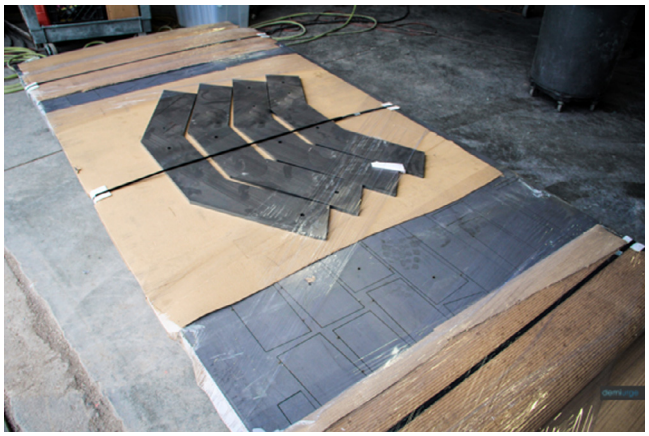

Fig. 14. Planar fabrication of stainless steel parts. *Source:* (Photo courtesy of Demiurge LLC).

Fig. 15. Welding process of the sculpture. *Source:* Photo courtesy of Demiurge LLC.

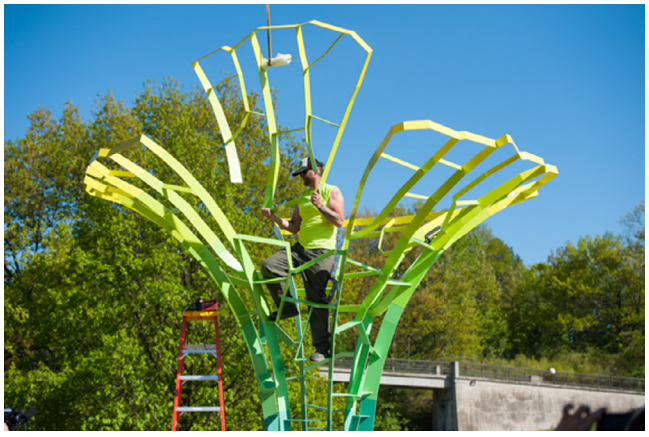

Fig. 16. Installation in site. *Source:* Photo by Adam Fenster, University of Rochester.

using high tension bolts. All the other pieces were raised and held in their position using a truck crane where they were joined to each other using bolts (Fig. 16). The adjacent edges of the groups were fabricated with half of the required material thickness to maintain the hierarchical geometry of the structure. During assembly, the pieces were combined like a jigsaw puzzle, first positioning opposite pieces, then inserting in-between pieces to maintain stability and balance.

6. Discussion

The morphogenetic extension of the two-dimensional leaf venation algorithm onto three-dimensional surfaces presents numerous technical challenges. Related examples of anisotropic pattern applications on manifold surfaces either show a similar implementation of the algorithm on mesh inputs with single curvature [40] or extension of the algorithm on hyperbolic surfaces without pattern anastomosis [41]. While it is possible to extend projection or UV mapping of the two-dimensional pattern onto mesh surfaces [12], growing emergent structures using three-dimensional geometric data poses restrictions on the type of input surfaces used. A strategy that needs to be further investigated is growing the input geometry simultaneously with the venation algorithm that requires further technical development to solve how the boundary and curvature of a growing input surface might restrict/influence the generation of the anisotropic structural pattern.

The hyperbolic surface for the venation algorithm is decided as a sculptural choice after carefully examining the preliminary test cases. This decision still yielded technical issues in the further development of the Calyx project as the generated geometry of the sculpture had to be simplified to produce a seamless node network. While the geometry optimization for two and three-legged node networks on 2d manifold surfaces can be achieved with the described numerical optimization method, this process requires the transformation of the anisotropic pattern into closed polygons that can be turned into a Delaunay triangulation to store adjacency and offset information for vertices [39].

During the design development of Calyx, the geometric challenges of the venation algorithm were solved with various computer-aided approaches spanning different software applications. The biomimetic approach of extending generative venation patterns for the design of custom structural objects currently serve for aesthetic pattern making and branching morphogenesis, while the extension of biomimetic fabrication, construction and assembly protocols need to be investigated [17]. For Calyx, extending the biomimicry argument over a hierarchical fabrication of the structure with calculated increments of material thicknesses was not possible, as the material choice for the outdoor sculpture was stainless steel and the material thickness and costs were optimized in consideration to the budget of the project. Although the fabrication and geometry optimization requirements have not been fully integrated into the morphogenetic process itself, the overall development of the project brought a general understanding of how anisotropic patterns on manifold surfaces could be abstracted into node network representations that can be geometrically optimized for planar fabrication.

7. Conclusion

This paper presented an interdisciplinary approach combining multi-faceted aspects of design, development, optimization, post-rationalization and fabrication. The morphogenetic aspects of venation patterns are investigated using computational tools that can generate structural networks with aesthetic and performative potential [4,13,14]. These patterns are explored on manifold surfaces with custom parametric densities [11] while developing a computer-aided design workflow and geometry optimization protocol that can be used for various digital fabrication applications. The extension of anisotropic patterns on surfaces presented

Fig. 17. Calyx on campus site.
Source: Photo by Adam Fenster, University of Rochester.

numerous technical problems since the generated structural network needed to built out of planar panels. To solve this issue, a post-rationalization and optimization protocol is discussed. For the former, the acquired anisotropic cells are first converted to a mesh by Delaunay triangulation of the overall structural network [39], before the normals of the mesh vertices are optimized to maintain the planarity of two-legged and three-legged nodes. The technical aspects of this algorithm show promise that could be extended to other complex geometric patterns and node networks with similar connectivity graphs. The main contributions of the presented work are summarized below:

– Development of a generative application of the venation algorithm on mesh surfaces with custom pattern densities

– Development of a geometry optimization protocol for the modelling of thickened panels derived from anisotropic patterns on two dimensional manifold surfaces with two or three degrees of node connectivity

– A computer-aided design workflow integrating various structural, geometric and fabrication parameters for the design and production of a sculpture

As a case study, Calyx brought numerous challenges within the domain of digital fabrication, generative design and geometry optimization. During the development of the project, the discussions among engineers, fabricators and computational designers yielded innovative solutions to deliver the sculpture within the financial and temporal requirements. A key factor in the successful completion of the project was the development of custom translation and optimization tools in Python and Mathematica. In Python, the venation patterns were transformed into meshes that contained both the cellular connectivity and surface normals. In Mathematica, this geometry was used to optimize the normal directions of each linear part to maintain planar connection of pieces. This post-rationalization process successfully enabled the planar fabrication of sculpture parts out of stainless steel.

In an age where interdisciplinarity and technology are becoming more integrated within the domain of design and engineering, computational designers are being tasked with exploring the frontier of developing innovative tools to solve complex problems. A key factor in the advancement of this domain is the creative ability for the development of necessary tools that tackle numerous technical problems encountered during projects. As a public artwork, Calyx brought numerous challenges that required negotiation and collaboration between different agents during project development (Fig. 17). Each separate application that was used during the project not only constrained the advancement of the project but also brought technical problems to the table such as geometry translation, optimization, post-rationalization, and digital fabrication requirements. Without computation, none of these aspects could have been tackled. This shows how viable these tools have become, to not only help communicate but also to innovate the technical aspects encountered during the project delivery process.

Declaration of competing interest

The authors declare that they have no known competing financial interests or personal relationships that could have appeared to influence the work reported in this paper.

Acknowledgements

The author thanks the digital fabricator, Demiurge LLC for their collaboration on the project, Jonathan McCann as manager of Campus Planning, Design and Construction Management (University of Rochester) and Allen Topolski (University of Rochester) for their support and Mark Luffel for his technical contribution on the project.

Funding

This work was developed as part of the University of Rochester campus public art program. The technical research was conducted in order to develop the artwork “Calyx”- a permanent installation in Rochester, New York.

Appendix A. Supplementary data

Supplementary material showing generative animations for the development of venation algorithm related to this article can be found online at https://doi.org/10.1016/j.cad.2021.103150.

References

[1] Austern G, Capeluto G, Grobman J. Rationalization methods in computer aided fabrication: A critical review. Autom Constr 2018;90. http://dx.doi.org/10.1016/j.autcon.2017.12.027.

[2] Krieg OD, Schwinn T, Menges A, Li J-M, Knippers J, Schmitt A, et al. Biomimetic lightweight timber plate shells: Computational integration of robotic fabrication, architectural geometry and structural design. In: Block Philippe, Knippers Jan, Mitra Niloy J, Wang Wenping, editors. Advances in architectural geometry 2014. Cham, CH: Springer; 2015, p. 109–25. http://dx.doi.org/10.1007/978-3-319-11418-7_8.

[3] Gerber DJ, Lin S-HE. Designing in complexity: Simulation, integration, and multidisciplinary design optimization for architecture. Simulation 2013;1–24.

[4] Hensel M. Performance-oriented architecture towards a biological paradigm for architectural design and the built environment. FORMakademisk 2010;3(1):36–56.

[5] Tamke M, Nicholas P, Zwierzycki M. Machine learning for architectural design: Practices and infrastructure. Int J Archit Comput 2018;16(2):123–43. http://dx.doi.org/10.1177/1478077118778580.

[6] Schling E, Kilian M, Wang H, Schikore J, Pottmann H. Design and construction of curved support structures with repetitive parameters. In: Hesselgren Lars, Olsson Karl-Gunnar, Kilian Axel, Malek Samar, Sorkine-Hornung Olga, Williams Chris, editors. AAG 2018. Advances in architectural geometry. 1. Auflage. Wien. Klein Publishing; 2018, p. 140–65.

[7] Mesnil, R. and Douthe, C. and Baverel, O. and Léger B. Morphogenesis of surfaces with planar lines of curvature and application to architectural design. Autom Constr 2018;95:129–41. http://dx.doi.org/10.1016/j.autcon.2018.08.007.

[8] Gerber D, Pantazis E, Wang A. A multi-agent approach for performance based architecture: design exploring geometry, user, and environmental agencies in façades. Autom Constr 2017;76:45–58. http://dx.doi.org/10.1016/j.autcon.2017.01.001.

[9] Shea K, Aish R, Gourtovaia M. Towards integrated performance-driven generative design tools. Autom Constr 2005;14(2):253–64.

[10] Manahl M, Stavric M, Wiltsche A. A ornamental discretisation of free-form surfaces: Developing digital tools to integrate design rationalisation with the form finding process. Int J Archit Comput 2012;10(4):595–612. http://dx.doi.org/10.1260/1478-0771.10.4.595.
[11] Gokmen S. A morphogenetic approach for performative building envelope systems using leaf venation patterns. In: Stouffs R, Sariyildiz S, editors. Computation and performance – proceedings of the 31st ECAADe conference, Vol. 1. Delft, The Netherlands: Faculty of Architecture, Delft University of Techology; 2013, p. 497–506.
[12] Runions A, Fuhrer M, Lane B, Federl P, Rolland-Lagan A-G, Prusinkiewicz P. Modeling and visualization of leaf venation patterns. ACM Trans Graph 2005;24(3):702–11.
[13] Roudavski S. Towards morphogenesis in architecture. Int J Archit Comput 2009;7(3):345–74.
[14] Menges A. Computational morphogenesis. In: Proceedings for 3rd international ASCAAD conference, Vol. 7, 2007. p 725-44.
[15] Carpo M. The digital turn in architecture 1992-2012. Chichester: Wiley; 2013.
[16] Hensel M, Menges A, Weinstock M. Emergence: morphogenetic design strategies, AD Vol. 74. Wiley Academy; 2004.
[17] Hensel M, Menges A, Weinstock M. Emergence morphogenetic design strategies, AD Vol. 74. Chichester: Wiley Academy; 2004, p. 3.
[18] Iasef Md R, Shuichi A. Computational design of a nature-inspired architectural structure using the concepts of self-similar and random fractals. Autom Constr 2016;66:43–58. http://dx.doi.org/10.1016/j.autcon.2016.03.010.
[19] Tepavcevic B, Stojaković V, Mitov D, Bajšanski I, Jovanović M. Design to fabrication method of thin shell structures based on a friction-fit connection system. Autom Constr 2017;84:207–13. http://dx.doi.org/10.1016/j.autcon.2017.09.003.
[20] Holzer D, Hough R, Burry M. Parametric design and structural optimisation for early design exploration. Int J Archit Comput 2007;5:625–43.
[21] Attar R, Aish R, Stam J, Brinsmead D, Tessier A, Glueck M, et al. Embedded rationality : a unified simulation framework for interactive form finding. Int J Archit Comput 2010;8:399–418. http://dx.doi.org/10.1260/1478-0771.8.4.399.
[22] Pottmann H, Liu Y, Wallner J, Bobenko A, Wang W. Geometry of multi-layer freeform structures for architecture. ACM Trans Graph 2007;26(3):65–es. http://dx.doi.org/10.1145/1276377.1276458.
[23] Scheible F, Dimcic M. Parametric engineering: Everything is possible. 2011.
[24] Scheurer F. Getting complexity organised using self-organisation in architectural construction. Autom Constr 2007;(16):78–85.
[25] Schleicher Simon, Lienhard J, Poppinga S, Speck T, Knippers J. A methodology for transferring principles of plant movements to elastic systems in architecture. Comput Aided Des 2015;60:105–17.
[26] Prusinkiewicz P, Lindenmayer A. The algorithmic beauty of plants. Springer-Verla; 1990.
[27] Menges Achim. OCEAN NORTH and Scheffler + partner international competition entry. New Czech National Library in Prague; 2021, http://www.achimmenges.net/?p=4452. [Accessed 20 June 2021].
[28] Hejnowıcz Z, Romberger J D. Growth tensor of plant organs. J Theor Biol 110(81984):93–114.
[29] Roth-Nebelsick A, Uhl D, Mosbugger V, Kerp H. Evolution and function of leaf venation architecture: a review. Ann Botany 2001;87:553–66.
[30] Sachs T. Cell polarity and tissue patterning in plants. Dev Suppl 1991;1:83–93.
[31] Dengler N, Kang J. Vascular patterning and leaf shape. Curr Opin Plant Biol 2001;4(1):50–6.
[32] Parish Yoav IH, Müller Pascal. Procedural modeling of cities. In: ProCeedings of the 28th annual conference on computer graphics and interactive tech-niques. New York, NY, USA: Association for Computing Machinery; 2001, p. 301–8. http://dx.doi.org/10.1145/383259.383292.
[33] Wong Michael, Zongker Douglas, Salesin David. Computer-generated floral ornament. In: Proceedings of the 25th annual conference on computer graphics and interactive techniques. 1998, http://dx.doi.org/10.1145/280814.280948.
[34] Bridson R. Fast poisson disk sampling in arbitrary dimensions, In Proceedings of ACM SIGGRAPH '07, 2007.
[35] sheng Wang Q, Ye J, Wu H, qing Gao B, Shepherd P. A triangular grid generation and optimization framework for the design of free-form gridshells. Comput Aided Des 2019;113:96–113. http://dx.doi.org/10.1016/j.cad.2019.04.005.
[36] Li Y, Liu Y, Wang W. Planar hexagonal meshing for architecture. In: IEEE transactions on visualization and computer graphics, Vol. 21, no. 1. 2015, p. 95–106. http://dx.doi.org/10.1109/TVCG.2014.2322367.
[37] Asterios Agkathidis, Brown Andre. Tree-structure canopy: A case study in design and fabrication of complex steel structures using digital tools. Int J Archit Comput 2013;11:87–104. http://dx.doi.org/10.1260/1478-0771.11.1.87.
[38] Lin Hongwei, Maekawa Takashi, Deng Chongyang. Survey on geometric iterative methods and their applications. Comput Aided Des 2018;95:40–51. http://dx.doi.org/10.1016/j.cad.2017.10.002.
[39] Eder Günther, Held M, Palfrader Peter. Parallelized ear clipping for the triangulation and constrained delaunay triangulation of polygons. Comput Geom 2018;73:15–23.
[40] Nervous System. Hyphae lamp. 2021, https://n-e-r-v-o-u-s.com/shop/generativeProduct.php?code=99. [Accessed 30 June 2021].
[41] Grant Associates. Supertrees. 2021, https://grant-associates.uk.com/projects/supertrees-gardens-by-the-bay. [Accessed 20 June 2021].